

Fuzzy Logic Trajectory Design and Guidance for Terminal Area Energy Management¹

Bradley T. Burchett²
 Department of Mechanical Engineering
 Rose-Hulman Institute of Technology
 Terre Haute, IN 47803

Abstract

The second generation reusable launch vehicle will incorporate sophisticated new guidance and control methods to increase the system's flexibility, in particular making it a practical vehicle for unmanned cargo missions. This project focuses on trajectory design and guidance for the Terminal Area Energy Management phase of flight where mathematically precise methods have produced limited results. Fuzzy Logic methods are used to make onboard autonomous gliding return trajectory design robust to the possibility of control surface failures, thus increasing the flexibility of unmanned gliding recovery and landing. Fuzzy inference systems are used to design the trajectory and provide guidance commands for the vehicle bank angle and negative z-axis acceleration. The design is validated using a high fidelity six degree of freedom simulation of the X-33 VentureStar.

Nomenclature

X_{HAC}	X runway coordinate of heading alignment cone center
ψ	heading angle with respect to runway (deg)
ϕ	bank angle (deg)
γ	flight path angle (deg)
g	gravity constant = 32.174 ft/s ²
V	forward velocity (ft/s)
x	vehicle cg distance from runway threshold (ft)
y	vehicle cg distance from runway centerline (ft)
h	vehicle cg distance above runway (ft)
N_z	vehicle z axis normal acceleration (g)
D	drag force (lb _f)
C_D	drag coefficient
ρ	atmospheric density (slug/ft ³)
S	vehicle frontal area (ft ²)
m	vehicle mass (slugs)
E_W	vehicle energy divided by weight (ft)
X_{MAX}	X_{HAC} value for maximum energy approach
X_{FTC}	Nominal value for X_{HAC}

X_{ALI}	X runway coordinate of baseline AutoLanding Interface (ALI) point
X_{MEP}	X runway coordinate for Minimum Entry point approach
r_{HAC}	radius of heading alignment turn (ft)
HAC	heading alignment cone
E_{MEP}	Energy over weight for minimum entry point approach
E_N	Energy over weight for nominal approach
SS	Energy over weight for small s-turn approach
SM	Energy over weight for medium s-turn approach
SL	Energy over weight for large s-turn approach
V_{HAC}	expected velocity at HAC initiation (ft/s)
ϕ_{AVG}	average bank angle during HAC turn (deg)
LN	Large Negative
MN	Medium Negative
SN	Small Negative
Z	Zero
SP	Small Positive
MP	Medium Positive
LP	Large Positive

Introduction

The second generation reusable launch vehicle will leverage many new technologies to make flight to low earth orbit safer and more cost effective. One important capability will be completely autonomous flight during reentry and landing, thus making it unnecessary to man the vehicle for cargo missions with stringent weight constraints. Implementation of sophisticated new guidance and control methods will enable the vehicle to return to earth under less than favorable conditions.

The return to earth consists of three phases—Entry, Terminal Area Energy Management (TAEM), and Approach and Landing. Entry is defined as taking the spacecraft from 190,000 ft to 90,000 ft above mean sea level. TAEM takes the spacecraft from 90,000 ft above mean sea level and Mach 3 to 10,000 ft and Mach 0.5 and aligns the craft with extended runway centerline. Approach and

¹This work was supported by NASA Contract number NAG81786.

²Assistant Professor, Member AIAA

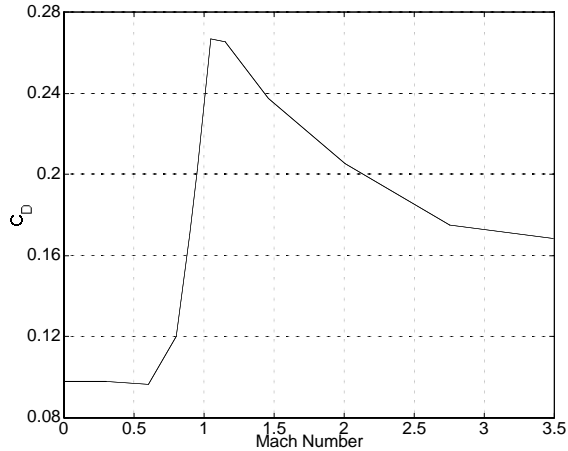


Figure 1: Simplified Model Drag Coefficient

Landing takes the vehicle from 10,000 ft to wheel stop on the runway. The Space Shuttle is programmed to fly all three phases of flight automatically, and under normal circumstances the astronaut-pilot takes manual control only during the Approach and Landing phase. The automatic control algorithms used in the Shuttle for TAEM and Approach and Landing have been developed over the past 30 years. They are computationally efficient, and based on careful study of the spacecraft’s flight dynamics, and heuristic reasoning. The gliding return trajectory is planned prior to the mission, and only minor adjustments are made during flight for perturbations in the vehicle energy state.

With the advent of the X-33 and X-34 technology demonstration vehicles, several authors investigated implementing advanced control methods to provide autonomous real-time design of gliding return trajectories, thus enhancing the ability of the vehicle to adjust to unusual energy states [1]– [6]. The bulk of work published to date deals primarily with the approach and landing phase of flight. Ref 1 focuses on the autoland trajectory where changes in heading angle are small and the distance to runway threshold is monotonically decreasing. Ref 2 proposes new methods to assess the robustness of autoland trajectories. Ref 3 shows results for the subsonic portion of TAEM. Ref 5 uses an adaptive-critic neural network approach to optimize trajectory design for the approach and landing phase of flight. Once again, the mathematics used are only applicable when the heading changes are small and the distance to the runway is monotonically decreasing.

This project focuses on the TAEM phase of flight where previously cited methods have produced limited results. Fuzzy Logic methods are used to autonomously design gliding return trajectories from the entry guidance

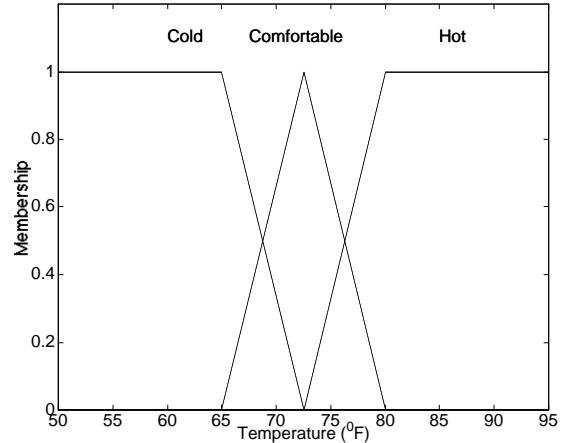


Figure 2: Membership Functions for Temperature Example

interface to autoland interface (ALI). In particular, the Fuzzy Logic method provides the capability of compensating for control surface failures by restricting the allowable bank angle used during the trajectory. Results of a high-fidelity simulation are presented for the entire TAEM phase from Mach 3 and 90,000 ft to ALI at approximately Mach 0.5 and 10,000 ft. The method provides a flyable trajectory with bank restricted to 36 deg. thus increasing the flexibility of unmanned gliding recovery and landing.

Simplified Model of Gliding Vehicle Dynamics

A simplified dynamic model of a gliding aircraft can be found by treating the vehicle as a point mass, and applying the Newton’s second law in the aircraft $y-z$ and $x-z$ planes separately. Considering the $y-z$ plane first, and assuming no acceleration in the z direction, Newton’s second law renders

$$L \cos \phi - mg = 0 \quad (1)$$

Which can be solved for lift L yielding

$$L = \frac{mg}{\cos \phi} \quad (2)$$

In the y direction we find

$$L \sin \phi = m \frac{V^2}{r} \quad (3)$$

Eq. 2 is then substituted for lift in Eq. 3, resulting in an expression for turn radius that is independent of aircraft size or type.

$$r = \frac{V^2}{g} \frac{1}{\tan \phi} \quad (4)$$

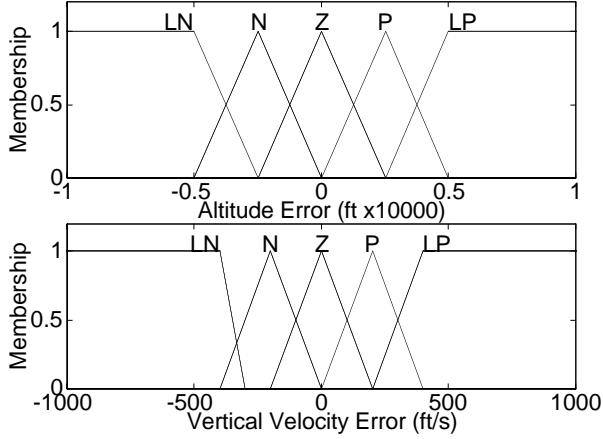


Figure 3: Partitioning of Altitude Error and Vertical Velocity Membership Functions

Now substituting $\psi^2 r = V^2/r$ in Eqn 4 and solving for turn rate ψ , results in the following:

$$\dot{\psi} = \frac{g}{V} \tan \phi \quad (5)$$

In the $x - z$ plane first show the force balance along the aircraft axis

$$L - mg \cos \gamma = m \frac{V^2}{r} = N_Z m \quad (6)$$

Solving for turn radius in the vertical plane yields

$$r = \frac{mV^2}{L - mg \cos \gamma} \quad (7)$$

Solving the Eq 6 for normal acceleration N_Z renders

$$N_Z = \frac{L}{m} - g \cos \gamma \quad (8)$$

Now substitute Eq 7 and $\dot{\gamma}^2 r = V^2/r$ into Eq 6 and solve for $\dot{\gamma}$

$$\dot{\gamma} = \frac{1}{V} \left(\frac{L}{m} - g \cos \gamma \right) \quad (9)$$

Finally, substituting Eq 8 into Eq 9 will eliminate lift and thus make the model independent of specific aircraft aerodynamic properties.

$$\dot{\gamma} = \frac{N_Z}{V} \quad (10)$$

The force-acceleration balance along the aircraft x axis results in an equation for forward velocity.

$$\dot{V} = -\frac{D}{m} - g \sin \gamma \quad (11)$$

Where drag D is given by

$$D = \frac{1}{2} \rho V^2 S C_D \quad (12)$$

Vertical Velocity Error		Altitude Error			
Error	LP	P	Z	N	LN
Z	LP	P	Z	N	LN
LN	Z	N	LN	LN	LN
N	P	Z	N	LN	LN
P	LP	LP	P	Z	N
LP	LP	LP	LP	P	Z

Table 1: Rules for Determining Negative Z Acceleration

By definition of heading angle and flight path angle, the aircraft position in x - y - h space is governed by Eqs. (13-15).

$$\dot{x} = V \cos \psi \quad (13)$$

$$\dot{y} = V \sin \psi \quad (14)$$

$$\dot{h} = V \sin \gamma \quad (15)$$

Atmospheric density is determined from the exponential model:

$$\rho = \begin{cases} 0.0023784722 (1 - 6.8789 \times 10^{-6} h)^{4.258} & h < 35332 \\ 0.00072674385 e^{-4.78 \times 10^{-5} (h - 35332)} & h \geq 35332 \end{cases} \quad (16)$$

Eqs. (5), (10), (11), and (13-16) provide a generic aerospace vehicle model where only the drag coefficient is aircraft specific. The coefficient of drag was taken to be a function of Mach number only and was approximated by the zero angle of attack portion of the drag table directly from a high-fidelity non-linear simulation of the X-33 Venturestar. These drag coefficient data are shown in Fig. 1. Induced drag was ignored which is probably the biggest weakness in the simplified model. The resulting model was programmed in Matlab / Simulink to serve as a test bed for rapid prototyping, tuning and testing of fuzzy inference systems for trajectory design and guidance.

Examining Eqs (5), (10), (11), and (13-16), it should be clear that vehicle ground track is controlled primarily by bank angle ϕ , the altitude is controlled by normal acceleration N_Z , and the dynamic pressure $\bar{q} = 1/2 \rho V^2$ is controlled by either changing the flight path angle γ or changing the coefficient of drag C_D , by extending drag devices.

The simplified dynamics were simulated in the Matlab/Simulink environment, and used for rigorous trial and error design of the fuzzy logic trajectory design and guidance algorithm. Although these dynamics appear overly simplified, they provided an adequate test-bed for development of the fuzzy rules. Flight path angle for an actual gliding return trajectory does not exceed 30 deg, and remains below 26 deg for half of the trajectory. Thus, ignoring the pitch effect on the horizontal flight path equations

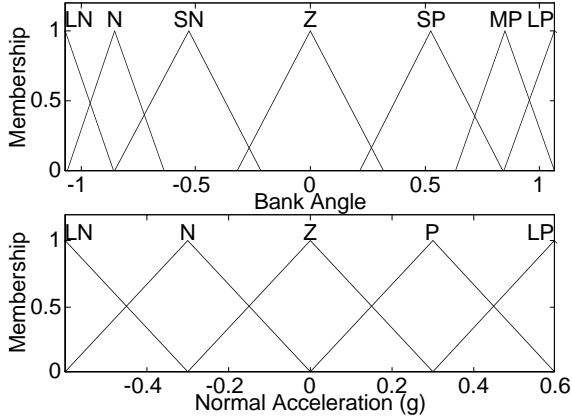


Figure 4: Partitioning of Bank Angle and Normal Acceleration Outputs

has little effect. Also, the inner-loop controller divides the guidance N_Z command by the cosine of current bank angle to compensate for the effect of bank. This justifies ignoring the effect of bank when computing the N_Z command to compensate for altitude. N_Z commands to compensate for altitude are limited to 0.6g to avoid exceeding the lift capabilities of the vehicle.

A Brief Introduction to Fuzzy Inference Systems

'Fuzzy Logic' and 'Approximate Reasoning' refer to a method of programming a computer to make decisions in an approximate way, similar to the way humans do. In a sense, it is an extension of 'crisp logic'. In crisp logic, a number either belongs to a set or does not. In fuzzy logic, a number may have partial membership in a set. For example, in crisp logic, the terms 'hot', 'comfortable', 'cold' must have crisp boundaries. Depending on the acclimation of the observer, we might assign boundaries such as

$$\begin{aligned}
 &\text{if } T < 65^{\circ}\text{F it is cold} \\
 &\text{if } 65^{\circ}\text{F} \leq T \leq 80^{\circ}\text{F it is comfortable} \\
 &\text{if } T > 80^{\circ}\text{F it is hot}
 \end{aligned}$$

This logic connects the qualitative adjectives hot, comfortable, and cold with specific quantities. However, since the adjectives are intended to be qualitative, and most human reasoning deals with 'thoughts' or 'ideas' rather than numbers, a better numerical representation of the adjectives is sought.

Fuzzy sets allow numbers to have partial membership in a set. Partial membership is determined by the height of the membership function at a particular numerical value. Membership functions can have any shape including triangular, trapezoidal, Gaussian, etc. For example, we might

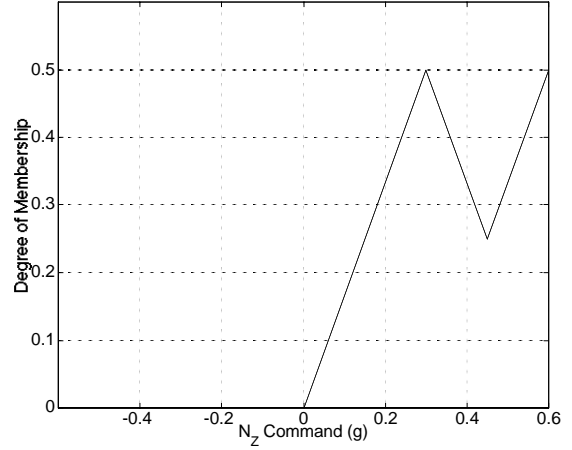


Figure 5: Aggregate Output Universe of Discourse for N example

fuzzify the previous example by assigning the membership functions shown in Fig. 2 to the adjectives used above. The range of possible values for a fuzzy input is termed the 'universe of discourse'. The 'truth value' is the synonymous with the 'degree of membership' of a particular number.

Now, if the temperature is 68°F , the term 'cold' has a truth value of 0.4, and 'comfortable' has a truth value of 0.6. Assignment of truth values is called 'fuzzification'.

A fuzzy inference system combines fuzzification with a set of if-then rules called the 'inference engine', and an output scheme called 'defuzzification' [7]. Consider the normal acceleration guidance commands inference systems as a somewhat richer example. The input membership functions are shown in Fig. 3. Suppose that the current altitude error is 1250 ft, and the current vertical velocity error is 200 ft/s. By examining the input membership functions, we see that $h_{err} = P$ and $h_{err} = Z$ each have a truth value of 0.5. vertical velocity error $\dot{h}_{err} = P$ has a truth value of 1. The rules for N_Z command are shown in Table 1. The first column is the vertical velocity error and the first row is the altitude error. All the rules have the form:

$$\text{if } h_{err} \text{ is } X \text{ and } \dot{h}_{err} \text{ is } Y \text{ then } N_Z \text{ is } Z$$

For instance, in the current illustration, one would enter the 'P' column for altitude error and the 'P' column for vertical velocity error and see that the directed output is 'LP'. This output would be given a weight equal to the minimum degree of membership of the relevant inputs, in this case 0.5. A second rule is also active, since $h_{err} = Z$ also has a non-zero degree of membership. The second rule is assessed by entering the 'Z' column and 'P' row of the table and reading N_Z is 'P' from the rule base. This

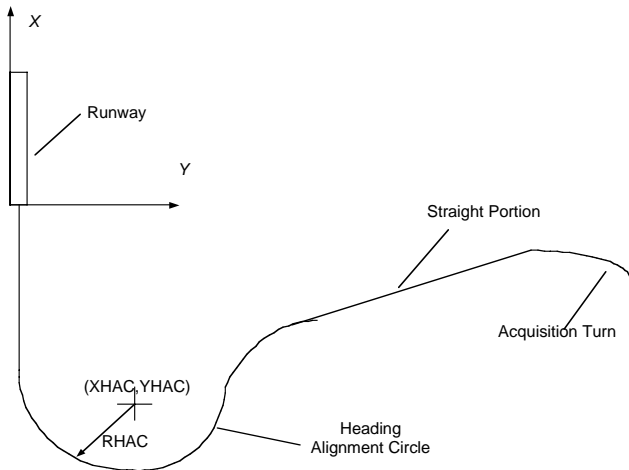


Figure 6: Baseline Trajectory Geometry

output membership function is also given a truth value of 0.5. The output membership functions for N_Z are shown in the lower half of Fig. 4.

Throughout this work, product implication is used. That is, the output membership function is multiplied by the truth value of the relevant rule. When more than one rule is active, maximum value aggregation is used. This is done by searching the universe of discourse of the output variable and assigning an output profile equal at each search point to the maximum of any implicated output membership function at that point. The aggregated output universe of discourse is shown in Fig. 5.

Once an aggregated output profile, a fuzzy quantity, is found, we must 'defuzzify' in order to provide a useful crisp number to the actuators. In this work centroidal defuzzification is used exclusively. Centroidal or center of gravity defuzzification is performed by treating the output profile as a series of point masses along a line, and finding the center of gravity along that line. It can be performed using the simple geometric average [8].

$$y_c = \frac{\int y\mu_A(y)dy}{\int \mu_A(y)dy}$$

For the current illustration, the resulting N_Z command is 0.3388g. Fuzzy Logic control has been used in a wide array of applications including approach and landing control of a light aircraft [9].

Fuzzy Logic Trajectory Design

Given the dynamics of Eqs. (5), (10), (11), and (13-16), and the wealth of knowledge from Shuttle heritage, we divided the trajectory design into three distinct channels; ground track, altitude, and dynamic pressure. For each

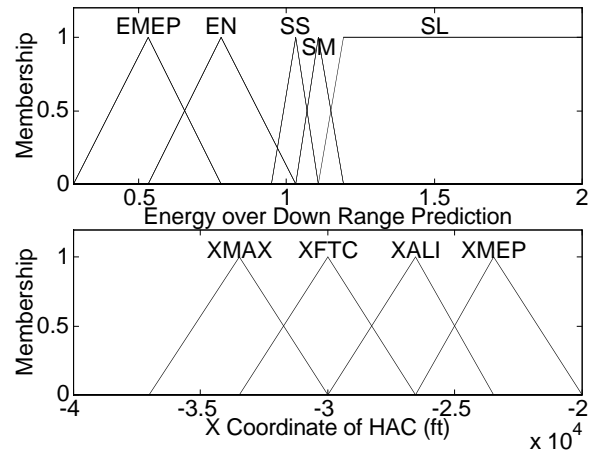


Figure 7: Energy over Down Range Prediction and X_{HAC} Membership Functions

channel, we constrained the trajectory to a shape that intentionally limits the number of parameters needed to describe it. Also, a number of acronyms used in this work follow directly from Shuttle heritage. All are defined in the Nomenclature section.

The ground path is patterned after a typical Tactical Air Navigation (TACAN) approach flown by military aircraft [11]. The basic geometry is shown in Fig. 6. The spacecraft flies a shortest direction acquisition turn to point directly to the station, a straight portion, and a base to final heading alignment cone (HAC) turn. Turning directly at the station follows allows the a definite transition to HAC phase, and provides that the HAC intercept may be flown based on the techniques used by military pilots. Each turn is designed as a circular arc. Finally, for each channel, important parameters defining the trajectory are determined through a Fuzzy Logic decision. The adjustable parameters in the horizontal channel are the heading alignment turn radius (Y_{HAC}), and position from the runway threshold (X_{HAC}).

The vertical trajectory is constrained by initial and final conditions. The spacecraft must reach the Auto-Land Interface (ALI) at approximately 10,000 ft above the runway, 20,000 ft from the runway threshold at a flight path angle depressed 30 deg from horizontal. To maintain continuity throughout the trajectory, the vertical path is defined as a cubic polynomial which intersects the ALI at the appropriate altitude and slope.

$$h_{ref} = c_4 R_{ALI}^3 + c_3 R_{ALI}^2 + c_2 R_{ALI} + h_{ALI}$$

Where R_{ALI} is the predicted ground track distance to ALI and h_{ALI} is the desired height at ALI and c_3 is an adjustable parameter allowing real-time updates of the reference vertical path to match off-nominal energy conditions.

Degree of Control Degradation	EMEP	EN	E_W/R_{ALI}		
			SS	SM	SL
Zero	XMEP	XALI	XFTC	XFTC	XMAX
Slight	XALI	XALI	XMAX	XMAX	XMAX
Moderate	XALI	XALI	XFTC	XFTC	XMAX
Severe	XALI	XALI	XMEP	XFTC	XFTC

Table 2: Rules for Determining XHAC

We designed a two-input three-output fuzzy inference system to determine X_{HAC} , Y_{HAC} and c_3 based on the spacecraft current energy state, and control surface health. The inputs are the quotient of energy over predicted down-range distance to ALI E_W/R_{ALI} , and an integer denoting the degree of control surface health. Energy is computed as the sum of kinetic and potential energy divided by weight, and has dimensions of length.

$$E_W = h + \frac{V^2}{2g} \quad (17)$$

Distance to ALI is computed using the expected ground track from the previous design iteration. The calculations are very similar to those used in Shuttle TAEM guidance. All design and guidance operations described in this paper are iterated at a rate of 2 Hz. The quotient of energy over distance to go is partitioned into five membership functions which are shown in the top half of Fig. 7.

Control surface health is given four possible integer values. Considering computation of X_{HAC} to be a two input fuzzy inference with five input membership functions on the first input (E_W/R_{ALI}) and four input membership functions on the second input (control surface health), results in twenty possible combinations for which we provide twenty total rules. The rules for X_{HAC} determination are shown in Table 2, where the degree of control surface degradation partitions are shown as row headings, and the partitions of E_W/R_{ALI} are shown as column headings. The associated output membership functions for the twenty rules are shown in the body of the table. The partitioning of the output universe of discourse for X_{HAC} is shown in the bottom half of Fig. 7.

The expected velocity in ft/s at HAC intercept is computed from a line fit model based on nominal trajectories. The lower limit of 820.97 ft/s is based on the dynamic pressure limit for stall at nominal HAC intercept altitude.

$$V_{HAC} = \max \left\{ \begin{array}{l} V - R_1 0.0326 \\ 820.97 \end{array} \right.$$

The expected turn radius for the HAC turn r_{HAC} can be computed from the expected velocity at HAC intercept V_{HAC} , and maximum bank ϕ_{avg}

$$r_{HAC} = \frac{V_{HAC}^2}{g \tan(\phi_{avg})} \quad (18)$$

Aero Failure	Max Bank (deg)	HAC radius (ft)
Zero	56	26,000
Slight	46	33,000
Moderate	36	41,000
Severe	26	50,000

Table 3: Default HAC Turn Radii

The HAC turn radius is set to the minimum of expected radius and value from Table 3. Center of gravity defuzzification is used in all fuzzy decisions in this paper. A second fuzzy inference system determines the maximum bank angle allowed (ϕ_{avg}) based upon the state of control surface health.

Bank Guidance Commands

The bank guidance commands are generated by a fuzzy inference system with seven inputs, 112 rules, and a single output. The conventional sub-phases of TAEM, which are acquisition, HAC turn, and pre-final 10, are used to limit the number of inputs which must be considered during a single iteration. For each sub-phase of TAEM, the system uses the relevant inputs to determine an appropriate bank angle. During the acquisition turn, the only input considered is turn angle to the HAC center, $\Delta\Psi_{aq}$ which is partitioned into five membership functions. In this phase, the fuzzy inference system acts as a proportional controller with five rules connected to the five output membership functions. That is, a 'large' difference in heading angle from HAC center will produce a 'large' bank angle in the appropriate direction. Likewise, as the difference in heading angle decreases to one-half degree, the guidance commands the spacecraft to roll out gradually. The acquisition turn ends when the spacecraft is pointed within one-half degree of the HAC center, or when it reaches a range of 1.85 HAC radii from the HAC center, to facilitate intercepting the HAC arc.

The basic rules for bank guidance are taken from techniques taught to military instrument pilots. The baseline geometry of the trajectory follows a typical TACAN approach where the aircraft is flown directly toward the station intercepts a circular arc around the station, then completes a base turn to final approach. The discussion which follows further illustrates the use of instrument flying techniques in designing the fuzzy inference system for bank commands.

In order to fly a constant radius turn around a station, the pilot turns the aircraft to position the station 'on the wing'. To maintain a constant radius, the pilot must consider both his distance from the station, and relative bearing. Thus, during the HAC turn, the relevant inputs are

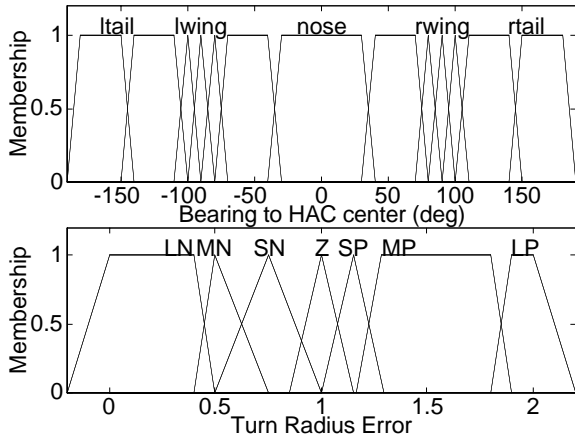


Figure 8: Partitioning of the Station Bearing and Turn Radius Error Inputs

turn radius error, bearing to the HAC center, and turn direction. Bearing to the HAC center is divided into thirteen membership functions with fine divisions near the wing where precise control is required. Turn radius error is expressed as a ratio of current turn radius over desired turn radius, and is partitioned into seven membership functions. These partitions are shown in Fig. 8. Eighty-nine rules are used during this phase. The rules corresponding to right turns are shown in Table 4 where the first column is bearing and the first row is turn radius error. Bearing uses the abbreviations 'nose' to denote the quadrant forward of the spacecraft, 'rf45' to denote the right forward quadrant, 'rf10' to mean approximately 10 deg forward of the right wing, 'wing', etc. Some rules do not consider turn direction, such as when approaching the station from far away. These rules are based on the author's own flight experience totaling more than 2000 hours in military jet aircraft, and relevant portions of Air Force Manual 11-217 Volume 1, *Instrument Flight Procedures* [11]. The rules for HAC sub-phase cause the spacecraft to execute an approximately 90 deg turn to intercept the HAC, then correct perturbations from the desired HAC radius until reaching pre-final transition. Pre-final transition is triggered when the spacecraft heading is within 45 deg of runway heading, and perpendicular distance from extended runway centerline is decreasing.

During pre-final phase the control objective is to position the aircraft on extended runway centerline, aligned with runway heading. Thus, the relevant inputs are the components of aircraft position and velocity perpendicular to runway centerline. We use fourteen rules to guide the aircraft aggressively back to runway. TAEM guidance ends when the altitude, runway Y coordinate, flight path angle, and dynamic pressure are all within approach and

Bearing to the Station	LP	MP	SP	Z	SN	MN	LN
nose	Z	N	LN	LN	LN	LN	LN
rf45	Z	Z	N	LN	LN	LN	LN
rf10	LP	LP	P	Z	N	LN	LN
rwing	LP	LP	P	P	Z	N	LN
ra10	LP	LP	LP	LP	Z	Z	N
ra45	LP	LP	LP	LP	P	Z	Z
tail	LP	LP	LP	LP	LP	LP	LP

Table 4: Default HAC Turn Radii

landing transition tolerances, or the spacecraft reaches a minimum altitude for approach and landing transition.

Note that the bank fuzzy inference system provides the proportion of available bank to be used as shown by the output membership functions in Fig. 4. The maximum available bank angle is determined as part of the acquisition turn trajectory planning. Maximum bank nominal values are shown in the middle column of Table 3. Bank guidance is computed as the product of maximum bank and the output of the bank fuzzy inference system. The bank commands are then smoothed by a first-order unity gain low-pass filter with cutoff frequency of 0.5 rad/s prior to transmission to the flight control system. This smoothing alleviates controller saturation and subsequent instability during abrupt changes in guidance caused by TAEM sub-phase changes.

Normal Acceleration Guidance

The negative z-axis acceleration guidance commands are determined by a fuzzy inference system with four inputs and 52 rules. The inputs are altitude error, vertical velocity error, dynamic pressure, and Mach number. The altitude error and vertical velocity error inputs are divided into five membership functions each. Thus, there are 25 rules for \bar{q} in the 'medium' range which are replicated for both subsonic and supersonic flight. These basic rules act as a proportional-derivative controller to align the spacecraft with the desired glidepath. The 25 basic rules are shown in Table 1 where the first column is the vertical velocity error and the first row is the altitude error.

The membership function partitions for altitude error and vertical velocity error are shown in Fig. 3. The membership function partitions for bank angle and normal acceleration output commands are shown in Fig. 4. Note that the negative z-axis acceleration guidance commands are limited to 0.6g to insure that the lift capability of the spacecraft is not exceeded.

During supersonic flight, the X-33 speed brake re-

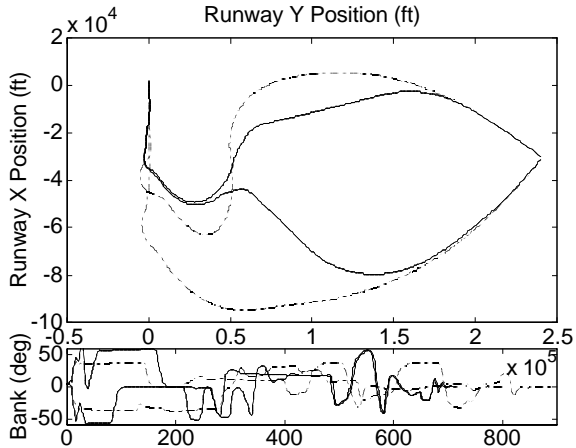


Figure 9: Vehicle Ground Track and Bank Angle for Various Initial Headings and Bank Restrictions

mains closed, and dynamic pressure is controlled by pitch attitude alone. During subsonic flight, no thrust is available, so pitch alone must be adjusted to avoid a stall condition. Thus, the following two rules are employed to keep the dynamic pressure within nominal limits for supersonic flight, and above the stall limit for subsonic flight.

if \bar{q} is low then N_z is LN

if \bar{q} is high and mach is super then N_z is P

Results

The fuzzy inference systems described above were rapidly prototyped, tuned, and tested using Matlab and the Fuzzy Logic Toolbox. The simplified three degree of freedom dynamics described earlier were programmed in Matlab and served as a realistic model of a reusable launch vehicle in the TAEM phase. The fuzzy inference systems described above were developed by formalizing a combination of the author’s own personal knowledge of instrument flying, and the expertise found in the existing Shuttle TAEM guidance. Extensive trial and error followed until the fuzzy algorithms could control the simplified dynamics to a satisfactory level. In particular, partitioning of the input space for each channel was done through careful observation of the state variables (altitude, forward velocity, vertical velocity, etc.) during high fidelity simulations with existing Shuttle TAEM guidance. That is, the terms ‘Large Positive’, ‘Medium Negative’, etc., were associated with numerical values by observing how much each input and output variable changes under existing guidance algorithms.

Variable and Units	Initial Condition Range Tested	Range Observed at ALI
Range to Runway (ft)	216000 < R < 280330	10101 < R < 12967
h (ft)	78000 < h < 88500	4784 < h < 4881
Mach	3.02	0.469 < Mach < 0.481
\dot{h} (ft/s)	-270	-449 < \dot{h} < -214
Ψ (deg)	236 < ψ < 297	356.6 < ψ < 5.6
γ (deg)	-6.16	-24.4 < γ < -28.8

Table 5: Initial Conditions Tested and ALI Envelope Demonstrated

Although the X-33 program has been cancelled, the high-fidelity models and simulations that were built as part of the program are unique in their maturity and utility. X-33 is currently the only vehicle that can be simulated in all phases of flight on the MAVERiC simulation package. After obtaining satisfactory results that demonstrated robustness to varying initial conditions and deg of control surface health, the fuzzy systems were integrated with the high fidelity six degree of freedom simulation known as MAVERiC. Limited further tuning was required to replicate the results obtained in Matlab. Since the initial design and tuning uses such a rough model, the same guidance laws should be readily adaptable to the next generation re-usable launch vehicle.

The ground track and bank angle of four high fidelity simulations are shown in Fig. 9. The solid lines represent the trajectory with full flight control authority. Dotted lines represent the trajectory when flight controls are degraded such that bank angle is limited to 36 deg. The axes on the ground track plot do not have equal scaling allowing differences to be emphasized. The four cases shown represent the limits on initial heading to reach a successful landing. Varying the heading by 30 deg, creates an energy initial state lower than nominal since maneuverability is limited at TAEM initiation, and the vehicle must fly a significantly longer ground track to turn back. The actual maximum bank used during degraded flight is 38.44 deg. All four cases plotted reach a successful landing at 1500 to 2500 ft from the runway threshold and within 33.64 ft of runway centerline.

At least twelve additional cases were run to test the limits on initial range from runway and altitude, as well as to repeat the initial heading range test for various degrees of maneuver restriction. The initial conditions tested are displayed in Table 5. The initial and final heading angle are shown as a compass heading with respect to runway heading. Thus the range observed at ALI is actually from 3.4 degrees left of runway heading to 5.6 degrees right of runway heading. The envelope for successful AutoLand Interface is defined by the maximum possible perturbation that existing Shuttle AutoLand guidance can tolerate at ALI and still reach a successful landing. This envelope observed throughout all testing is shown in Table 5.

Fig. 10 shows the corresponding altitude profiles.

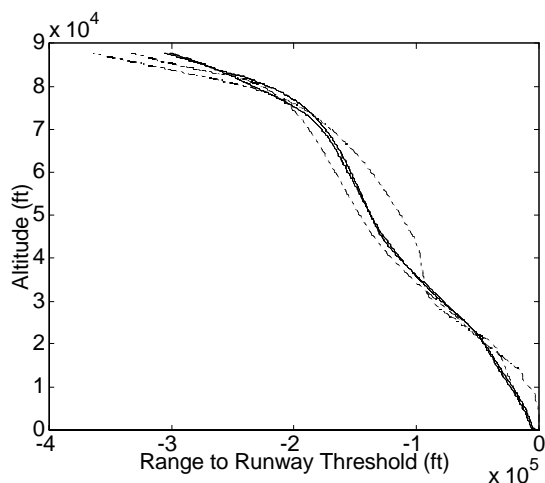


Figure 10: Vehicle Altitude for Various Initial Headings and Bank Restrictions

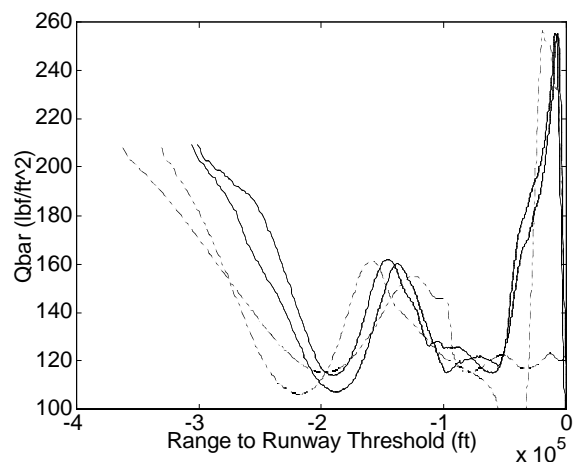


Figure 11: Dynamic Pressure for Various Initial Headings and Bank Restrictions

Both full control cases and one of the degraded cases converge to the desired ALI conditions. The degraded case with initial heading furthest to the right reaches ALI very steep and high.

The corresponding dynamic pressure profiles are shown in Fig. 11. Note that all trajectories stay within the nominal limits of 100 to 300 lbf/ft^2 .

Additional tests were run to vary the initial distance from ALI, and the initial altitude. The minimum altitude at TAEM interface for successful landing was found to be 78000 ft. The maximum altitude was found to be 88500 ft. This does not represent an improvement over current guidance.

One fascinating discovery is that the fuzzy inference systems have complimentary effects on each other although each channel was designed separately. For example, for a case with flight control limitations, and nominal initial energy, the trajectory designer will direct a wide radius HAC. The ground track predictor then computes a longer than normal ground track. Subsequently, the normal acceleration guidance keeps the flight path angle shallow during the acquisition phase of flight. This is then advantageous to the bank guidance since the spacecraft will reach subsonic flight sooner, and will thus be ready to intercept the HAC.

Conclusions

Fuzzy logic control is extremely powerful for control of complex systems without precise models. Several fuzzy inference systems have been designed by application of the knowledge base from Shuttle TAEM guidance and the author's own flight experience. These fuzzy systems were tuned by trial and error on a very simple set of dynamics,

then programmed into a high-fidelity six degree of freedom simulation. Although the each channel of the fuzzy guidance system was designed separately, and tuned on dynamics where the axes were completely de-coupled, the new guidance system still performed well on the high fidelity simulation where the dynamics are very realistic. In fact, the separate channels show complimentary effects. The high fidelity simulations demonstrate an ability to autonomously design and fly gliding return trajectories for varying initial energy conditions and stringent maneuver restrictions.

References

- [1] Barton, G. H., "Autolanding Trajectory Design for the X-34," AIAA Paper No 99-4161, 1999.
- [2] Barton, G. H., "New Methodologies for Assessing the Robustness of the X-34 Autolanding Trajectories," *Advances in the Astronautical Sciences*, Volume 107 Guidance and Control 2001, pp. 193-214.
- [3] Girerd, A., Barton, G., "Next Generation Entry Guidance—Onboard Trajectory Generation for Unpowered Drop Tests," AIAA Paper No 2000-3960, August, 2000.
- [4] Girerd, A., "Onboard Trajectory Generation for the Unpowered Landing of Autonomous Reusable Launch Vehicles," S. M. Thesis, Massachusetts Institute of Technology / Charles Stark Draper Laboratory T-1390, 2001.
- [5] Grantham, K. "Adaptive Critic Neural Network Based Terminal Area Energy Management / Entry Guidance," AIAA Paper 2003-0305, January, 2003.
- [6] Grubler, A. C., "New Methodologies for Onboard Generation of Terminal Area Energy Management Trajectories for Autonomous Reusable Launch Vehicles," S. M.

Thesis, Massachusetts Institute of Technology / Charles Stark Draper Laboratory T-1401, 2001.

[7] Lee, C. C., “Fuzzy Logic in Control Systems: Fuzzy Logic Controller—Part I,” *IEEE Transactions on Systems, Man, and Cybernetics*, Vol. 20, No. 2, 1990, pp. 404-417.

[8] Jamshidi, M., dos Santos Coelho, L., Krohling, R., and Fleming, P., *Genetic Algorithms in Robust Control* CRC Press, Boca Raton, FL, 2003, p. 199.

[9] Larkin, L. I., “A Fuzzy Logic Controller for Aircraft Flight Control,” *Industrial Applications of Fuzzy Control*, M. Sugeno, Ed., Elsevier Science Publishers, North Holland, 1985, pp. 87-103.

[10] Moore, T. E. “Space Shuttle Terminal Area Energy Management,” NASA Technical Memorandum 104744, Lyndon B. Johnson Space Center, November, 1991.

[11] Air Force Manual 11-217 Volume 1, *Instrument Flight Procedures*, 29 December 2000, <http://afpubs.hq.af.mil>